Quantum Electronics **43** (11) 1029–1036 (2013) ©2013 Kvantovaya Elektronika and Turpion Ltd

NONLINEAR OPTICAL PHENOMENA

PACS numbers: 42.65.Re; 42.65.Sf; 42.70.Qs; 42.81.Dp
DOI: 10.1070/QE2013v043n11ABEH015228

Dynamics of optical pulses in waveguides with a large self-steepening parameter

V.M. Zhuravlev, I.O. Zolotovskii, D.A. Korobko, A.A. Fotiadi

Abstract. **We study the dynamics of a high-energy laser pulse in dispersive optical media with large values of self-steepening. We consider the formation of soliton-like peaks at the front of the envelope in such media with anomalous dispersion. We show the possibility of realisation of a medium based on a photonic crystal waveguide with a very large absolute value of the self-steepening parameter in a certain frequency range.**

Keywords: *shock waves of the envelope, high-power laser pulses, self-steepening, photonic crystal waveguides.*

1. Introduction

The phenomenon of shock waves of laser pulse envelopes was first investigated by L.A. Ostrovskii almost 50 years ago [1, 2]. He showed that the dependence of the group velocity on the intensity of a high-power laser pulse propagating in a medium leads to a nonlinear transformation of its shape and to an increase in the steepness of its edge (leading or trailing edge as a function of the sign of the Kerr nonlinearity dispersion). As a result, a shock wave of the laser pulse envelope can be generated, which resembles the process of formation of shock waves in acoustics [3].

Dynamics of shock wave formation in nonlinear media has been considered in detail in many papers [4–12]. However, the appearance of new optical materials – photonic crystal fibres [13–15] and composite materials with giant nonlinearities, producing conditions for plasmon resonance [16–18] – makes it relevant to consider the dynamics of high-power laser pulses in media with a large self-steepening parameter. In waveguide systems of this type, self-steepening can take giant values as compared to 'conventional' optical materials (e.g. silica fibres). Furthermore, we will consider the problem of realisation of a waveguide having not only positive but also negative self-steepening, which leads to steepening of the leading edge of the laser pulse (unlike the case of a positive parameter when the trailing edge is deformed).

V.M. Zhuravlev, I.O. Zolotovskii, D.A. Korobko Ulyanovsk State University, ul. L. Tolstogo 42, 432700 Ul'yanovsk, Russia; e-mail: rafzol.14@mail.ru;
A.A. Fotiadi Université de Mons, 20, place du Parc, B7000 Mons, Belgique; Ulyanovsk State University, ul. L. Tolstogo 42, 432700 Ul'yanovsk, Russia; e-mail: fotiadi@mail.ru

Received 30 April 2013; revision received 11 July 2013
Kvantovaya Elektronika **43** (11) 1029–1036 (2013)
Translated by I.A. Ulitkin

Generation of shock waves with a very steep leading edge may be of considerable practical interest. Thus, in one of the first methods of high-power pulse shortening, the authors of [19, 20] suggested using conventional optical amplifiers as compressors in a strongly inverted active medium. The application of this scheme proved difficult, because if the pulse has a sloping front, amplification of the leading edge of the pulse fed to the amplifier will not lead to its shortening, but on the contrary, can cause considerable broadening. In view of this, the amplifier is placed behind a device (such as a Kerr or a Pockels cell), which 'cuts' the front of the pulse fed to the amplifier. Thus, for a pulse to be shortened during the amplification process, it is highly desirable to cut off parts of its low-intensity leading edge so that they could not 'deplete' the active medium before the arrival of the envelope maximum. To this end, it is important to shape the rising edge of the pulse in the form of a step; then, the front part of the pulse will receive most of the energy stored in the amplifier. As a result, we can state that the possibility of formation of shock waves at the leading edge of the pulse is achieved without additional cut-off devices in the implementation of the regime combining amplification and temporal compression for high-power laser pulses in the active medium.

We should also mention the related phenomenon that has recently attracted a lot of attention – wave packets called rogue waves in the literature [21–24]. Their specific feature includes the deformation of the wave front (the so-called optical tsunami [25, 26]). All of the above-said demonstrates the importance of studying the dynamics of high-power laser pulses in media with a large self-steepening parameter, which can be both positive and negative.

2. General model of shock wave formation in inhomogeneous optical fibres

Propagation of a wave packet in an optical medium with the Kerr nonlinearity is described by the equation [27]

$$\frac{\partial^2 E}{\partial z^2} - \frac{1}{c^2}\frac{\partial^2 E}{\partial t^2} + \mu_0 \frac{\partial^2 P_{\rm L}}{\partial t^2} = -\mu_0 \frac{\partial^2 P_{\rm NL}}{\partial t^2}. \qquad (1)$$

Here, $E(z,t)$ is the electric field of the wave packet, which can be expressed in terms of the complex slowly varying amplitude: $E(z,t) = |A(z,t)|\exp\{\mathrm{i}[(\beta(\omega,z)-\beta_0)z-(\omega-\omega_0)t]\}$; $P_{\rm L}$ and $P_{\rm NL}$ are the linear and nonlinear Kerr polarisation components, respectively; β_0 and ω_0 are the propagation constant and the carrier frequency of the packet; and μ_0 is the permeability of free space. For wave packets with a duration $\tau_0 \gg \tau_{\rm NL}$

(in the case of a quasi-static nonlinear response), the expression for the nonlinear Kerr polarisation

$$P_{\rm NL} = \frac{3}{2}\varepsilon_0\chi^{(3)}|A|^2 A\exp[{\rm i}(\beta_0 z - \omega_0 t)]$$

is valid, where $\tau_{\rm NL}$ is the characteristic time of the nonlinear response of the medium; $\chi^{(3)}$ is the Kerr dielectric susceptibility; and ε_0 is the dielectric constant of the vacuum. In the first order of smallness in the parameter $\tau_{\rm NL}/\tau_0$, the nonlinear source in (1) is described by the expression [28]

$$\frac{\partial^2 P_{\rm NL}}{\partial t^2} = -\frac{3}{2}\frac{\omega_0^2}{c^2}\left[\chi^{(3)}|A|^2 A - {\rm i}\left(\frac{2\chi^{(3)}}{\omega_0} - \frac{\partial\chi^{(3)}}{\partial\omega}\right)\frac{\partial}{\partial t}(|A|^2 A)\right]$$

$$\times\exp[{\rm i}(\beta_0 z - \omega_0 t)]. \qquad (2)$$

Consider the radial field distribution $U(r)$ in the waveguide in the plane perpendicular to the propagation direction [29]

$$\tilde{E}(\boldsymbol{r},t) = E(z,t)\,U(r,\phi) = U(r)\cos(m\varphi)$$

$$\times A(z,t)\exp[{\rm i}(\beta_0 z - \omega_0 t)],$$

where m is the azimuthal mode index. The transverse profile of the mode field $U(r)$ satisfies the wave equation

$$\frac{{\rm d}^2 U}{{\rm d}r^2} + \frac{1}{r}\frac{{\rm d}U}{{\rm d}r} + \left\{\left[\frac{\omega}{c}n(r)\right]^2 - \beta^2 - \frac{m^2}{r^2}\right\}U = 0. \qquad (3)$$

In the following we imply that we consider the propagation of the wave packet in a single-mode azimuthally symmetric case ($m = 0$). Through the distribution $U(r)$ we define the parameter $S_{\rm eff}$, i.e., the effective mode area:

$$S_{\rm eff} = 2\pi\left(\int_0^\infty |U(r)|^2 r{\rm d}r\right)^2 \Big/ \left(\int_0^\infty |U(r)|^4 r{\rm d}r\right).$$

In the general case, this parameter may be varied along the length of the waveguide. We also introduce the following notations, which we will use below:

$$n^{(2)} = \frac{3\chi^{(3)}}{8n},\ R = \frac{n^{(2)}\omega_0}{cS_{\rm eff}}.$$

Here, n is the linear refractive index; $n^{(2)}$ is the cubic Kerr nonlinearity parameter; and R is the coefficient of nonlinearity (in $\rm W^{-1}\,m^{-1}$), which can also depend on z. Using the standard procedure [27, 28], from the equation (1) we can obtain the equation for the slowly varying amplitudes $A(z, t)$, which in the associated coordinate system moving with the group velocity $u_{\rm g}(z) = (\partial\beta/\partial\omega)^{-1}_{\omega=\omega_0}$ has the form

$$\frac{\partial A}{\partial z} - \frac{{\rm i}D}{2}\frac{\partial^2 A}{\partial\tau^2} + {\rm i}R|A|^2 A + \mu\frac{\partial}{\partial\tau}(|A|^2 A) = 0, \qquad (4)$$

where

$$\tau = t - \int_0^z {\rm d}z/u_{\rm g}(z)$$

is the time in the associated coordinate system, and $D(z) = (\partial^2\beta/\partial\omega^2)^{-1}_{\omega=\omega_0}$ is the group-velocity dispersion (GVD). The self-steepening parameter μ will play below an important role. In the general case, this parameter also depends on the longitudinal coordinate z, which can be written in the form [28, 30]

$$\mu = \frac{2n^{(2)}}{cS_{\rm eff}} - \frac{\omega_0}{c}\frac{\partial}{\partial\omega}\left(\frac{n^{(2)}}{S_{\rm eff}}\right). \qquad (5)$$

When the term related to this parameter is taken into account in (4), there appears a nonlinear correction to the wave group velocity, which is proportional to the second term in the expression

$$\frac{\partial}{\partial\tau}(|A|^2 A) = A\frac{\partial|A|^2}{\partial\tau} + |A|^2\frac{\partial A}{\partial\tau}.$$

The dependence of the group velocity of the wave on its amplitude is a characteristic feature of the formation of a shock wave of the envelope. When $\mu > 0$, the maximum of the pulse envelope propagates with a velocity that is less than the group velocity $u_{\rm g}$ of the wave packet in a medium, which means that the maximum is displaced to the tail of the wave packet, resulting in an increase in the slope of the trailing edge of the pulse. If $\mu < 0$, a shock wave can be produced at the leading edge of the pulse.

Let us illustrate this by the well-known example [4], in which we neglect the dispersion effects. This approximation is quite correct for sufficiently long optical pulses with the spectral width

$$\Omega \approx \frac{1}{\tau_0} \ll \frac{\mu|A|^2}{|D|}.$$

We represent the solution of equation (3) in the form

$$A(z,t) = \rho(z,t)\exp[{\rm i}\varphi(z,t)], \qquad (6)$$

where ρ and φ are the real amplitude and the phase of the wave packet. Neglecting the dispersion term and separating the real and imaginary parts in equation (4), for the amplitude of the wave packet we obtain the equation:

$$\frac{\partial\rho}{\partial z} + 3\int_0^z \mu(\xi){\rm d}\xi\,\rho^2\frac{\partial\rho}{\partial\tau} = 0. \qquad (7)$$

We analyse the solution of the derived equation (7) by the example of an initial Gaussian pulse:

$$\rho(\tau,0) = \rho_0\exp\left(-\frac{\tau^2}{2\tau_0^2}\right).$$

The solution to the equation for the amplitude $\rho(\tau, z)$, which determines the shape of the pulse, can be written in the implicit form:

$$\rho(\tau,z) = \rho_0\exp\left\{-\left[\tau - 3\rho^2\int_0^z \mu(\xi){\rm d}\xi\right]^2 \Big/ (2\tau_0^2)\right\}. \qquad (8)$$

Given the definition of time in the moving coordinate system for the velocity of the wave packet envelope maximum $u_{\rm m}$, the relation

$$u_{\rm m} = z\left[\int_0^z u_{\rm g}^{-1}(\xi){\rm d}\xi + 3\rho^2\int_0^z \mu(\xi){\rm d}\xi\right]^{-1} \qquad (9)$$

is valid. In the general case, the value of u_m is a complex function of the coordinate z. In the particular case of a uniform fibre (i.e., when μ = const, u_g = const), the expression for the velocity of the envelope maximum takes the known form [4]:

$$u_m = \frac{u_g}{1 + 3\mu u_g \rho_0^2}. \quad (10)$$

It is obvious that in the linear approximation (i.e. for a low-power pulse when $\mu\rho_0^2 \to 0$) the velocity of the envelope maximum coincides with the group velocity of the pulse.

To determine the shape of the pulse in a nonlinear amplifying medium, relation (8) can be conveniently represented as

$$\tau = 3\rho^2 \int_0^z \mu(\xi)\,d\xi \mp \tau_0 \sqrt{2\ln(\rho_0/\rho)}, \quad (11)$$

where the sign '–' refers to the front of the pulse, and the sign '+' – to the tail. The steepening of the pulse front finally leads, at some length L_b, to the formation of the gap, to which the condition $|\partial\rho/\partial\tau| \to \infty$ corresponds, i.e., the shock wave of the envelope is produced. From (11) we can obtain an implicit relation of the length L_b of the shock wave formation with the parameters of the fibre and the pulse coupled into it:

$$\int_0^{L_b} \mu(z)\,dz = \mathrm{sign}\langle\mu\rangle \frac{\tau_0\sqrt{e/2}}{3\rho_0^2}.$$

In the case of a uniform amplifier (μ = const) from this relation we can obtain the well-known expression [28]

$$L_b = \frac{\tau_0\sqrt{e/2}}{3|\mu|\rho_0^2}.$$

Note that all the above results can be also used for an active fibre with the gain $G(z)$ described by the equation

$$\frac{\partial A}{\partial z} - \frac{iD}{2}\frac{\partial^2 A}{\partial\tau^2} + iR|A|^2A + \mu\frac{\partial}{\partial\tau}(|A|^2A) = GA. \quad (12)$$

In this case, equation (4) with the effective coefficients

$$\tilde{R}(z) = R(z)\exp\left[2\int_0^z G(\xi)\,d\xi\right], \quad \tilde{\mu}(z) = \mu(z)\exp\left[2\int_0^z G(\xi)\,d\xi\right]$$

remains valid for the amplitudes $\tilde{A}(z,\tau)$ related to the initial amplitudes as follows:

$$A(z,\tau) = \tilde{A}(z,\tau)\exp\left[\int_0^z G(\xi)\,d\xi\right].$$

3. Formation of shock waves in waveguides with dispersion. Results of numerical simulation

The above relations provide a simplified schematic picture of the formation of shock waves in optical waveguides. Meanwhile, the GVD has a significant impact on the transformation of the pulse, which is described by equation (4). Even if at the initial stage the pulse duration was significant and the GVD effects could be ignored, with steepening of the front pulse, i.e., at $\partial|A|/\partial\tau \to \infty$, the dispersive spreading starts playing a major role: when a shock wave is produced, the spectral width of the pulse increases, which makes dispersion effects more significant. The spread in the velocity due to dispersion limits the slope of the pulse front.

Known are the exact solutions of equation (4) with constant coefficients that describe the propagation of kinks ('steps') [5] of radiation and soliton-like pulses in the limit $\mu \to 0$, undergoing a transition into fundamental solitons of the nonlinear Schrödinger equation (NSE) [6–8]. Exact analytical solutions for pulses with energies exceeding the energies of the fundamental soliton, i.e., in the case $\rho_0^2 > D/(R\tau_0^2)$ are unknown, and hence we have to restrict ourselves to the numerical solution of equation (4). We have performed the numerical analysis of the evolution of the initial pulse with the amplitude $A_0(t) = \sqrt{P_0}\cosh(\tau/\tau_0)$, duration τ_0 = 25 ps and power P_0 = 115 W in a waveguide with anomalous ($D < 0$) and normal ($D > 0$) dispersion. The results are shown in Figs 1 and 2. Note that in the simulation we used both positive and negative values of the self-steepening parameter $|\mu| = 10^{-14}$ W^{-1} m^{-1} s. The possibility of obtaining such large values of μ of different signs in photonic crystal (PC) waveguides is discussed below in Section 4. We should also add that the parameters of nonlinearity R and dispersion D used hereafter are slightly higher than the standard values for silica fibres, but achievable in the PC waveguides. For comparison, we also present the results in the dispersion-free case.

One can see from Fig. 1 that the pulse during its propagation becomes asymmetrical with a steep rising or falling edge, depending on the sign of μ. The spectrum of the pulse (Fig. 2) considerably broadens towards higher or lower frequencies as a function of acceleration ($\mu < 0$) or slowing-down ($\mu > 0$) of the pulse maximum. The comparison of the spectrum with the

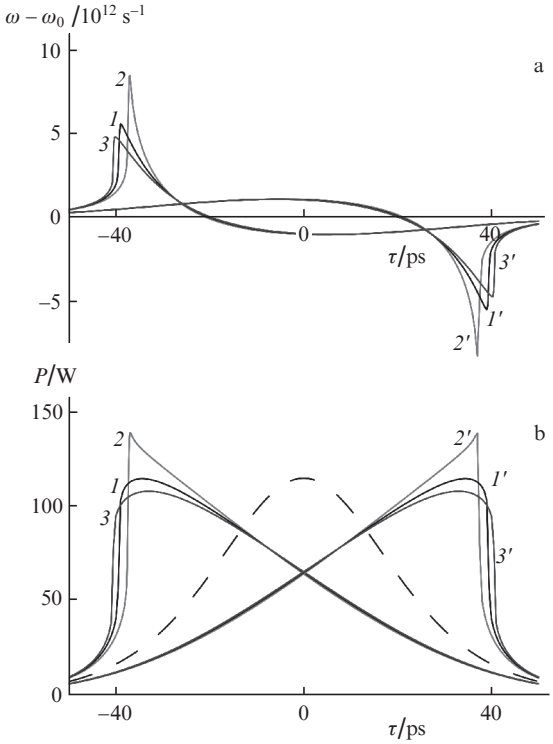

Figure 1. Formation of a shock wave: (a) change in the instantaneous frequency and (b) pulse envelopes after propagation in a 10-m-long waveguide with the parameters R = 0.05 W^{-1} m^{-1}, μ = (*1–3*) -10^{-14} and (*1′–3′*) 10^{-14} W^{-1} m^{-1} s, D = (*1*, *1′*) 0, (*2*, *2′*) -7×10^{-26} and (*3*, *3′*) 5×10^{-26} s^2 m^{-1}. The dashed curve is the envelope of the initial pulse.

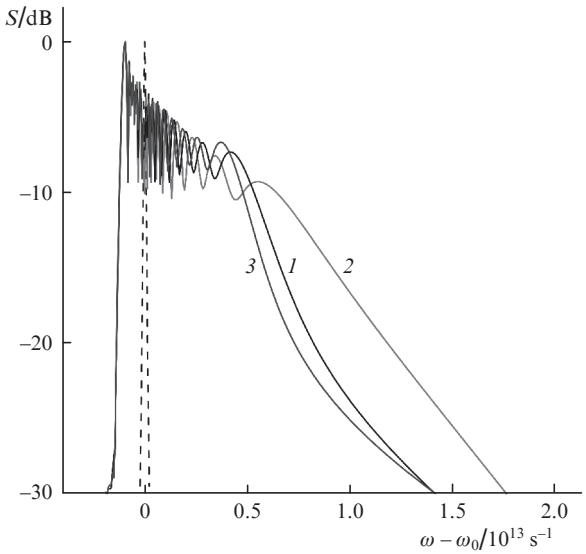

Figure 2. Spectrum of a shock wave upon steepening of the leading edge of the pulse passing through a 10-m-long waveguide with the parameters $R = 0.05\ \mathrm{W^{-1}\ m^{-1}}$, $\mu = -10^{-14}\ \mathrm{W^{-1}\ m^{-1}\ s}$, $D = (1)\ 0$, $(2)\ -7\times10^{-26}$ and $(3)\ 5\times10^{-26}\ \mathrm{s^2\ m^{-1}}$. The dashed curve is the spectrum of the initial pulse.

time-dependent instantaneous frequency (Fig. 1a) shows that the broadening of the spectrum is due to the shift of the frequency of the steepest part of the pulse front. In the region of normal dispersion the front is shifted away from the initial centre of the pulse, but its frequency shift is smaller than that in the region of anomalous dispersion. In the case of anomalous dispersion, the maximum frequency shift is observed near the pulse maximum, which is consistent with the analytical solutions of equation (4). It is known that the exact soliton solutions of this equation have a specific phase modulation [6–8]

$$\varphi_\tau \propto -\frac{3}{2}\mu|A(\tau)|^2 + \Delta u,$$

where Δu is the difference between the velocity of the soliton and the group velocity of the wave. Thus, we can assume that in the region of anomalous dispersion at the pulse front soliton-like frequency-modulated pulses are produced.

Consider in more detail the formation of the shock wave front. Note that the spreading of the front in the case of normal dispersion can be approximately described by the relation for the velocity of the pulse envelope maximum (10). Indeed, the change in the velocity of this maximum due self-steepening $\Delta u_\mathrm{m} \simeq 3\mu u_\mathrm{g}^2 P_0$ is compensated for by the dispersion change in its velocity that occurs due to the broadening of the pulse spectrum:

$$\Delta u_\mathrm{m} \approx \frac{\mathrm{d}u_\mathrm{g}}{\mathrm{d}\omega}\Delta\omega \simeq 3\mu u_\mathrm{g}^2 P_0.$$

Given the fact that $\mathrm{d}u_\mathrm{g}^{-1}/\mathrm{d}\omega = D$, we can estimate the duration of the steep front τ_f of the pulse in the case of normal dispersion:

$$\tau_\mathrm{f} \simeq \frac{D}{3\mu P_0}. \qquad (13)$$

Somewhat different is the steepening of the front in the case of anomalous dispersion. It is well known that propagating in a nonlinear medium with anomalous dispersion described by the NSE the pulse with an energy much higher than the energy of the fundamental soliton (N-soliton pulse, $N \gg 1$) is transformed into a set of short pulses that are close to the fundamental solitons. This is one of the manifestations of the specific nonlinear process of the modulation instability [27]. If, by analogy with the NSE, equation (4) is analysed for the stability of a permanent solution $A = A_0\exp(\mathrm{i}RA_0^2 z)$ to small harmonic perturbations, one can obtain that the term proportional to the parameter μ prevents the development of the modulation instability and stabilises the integrity of the pulse to some extent. Indeed, the expression for the gain of the small modulation at a frequency $\Omega = |\omega - \omega_0|$ can be written in the form [31]

$$g(\Omega) = 2\Omega\left[R|D|A_0^2 - \left(\frac{|D|\Omega}{2}\right)^2 - \mu^2 A_0^4\right]^{1/2}. \qquad (14)$$

It takes real values in the frequency band

$$\Omega < \Omega_\chi = \frac{2A_0}{|D|}(R|D| - \mu^2 A_0^2)^{1/2}$$

and reaches a maximum value

$$g_\mathrm{m} = 2A_0^2\left(R - \frac{\mu^2}{2|D|}A_0^2\right)$$

at a frequency

$$\Omega_\mathrm{m} = \sqrt{2}\,A_0\left(\frac{R}{|D|} - \frac{\mu^2 A_0^2}{2D^2}\right)^{1/2}.$$

Thus, self-steepening reduces the modulation gain and decreases the modulation instability bandwidth. At $\mu > (R|D|)^{1/2}/A_0$ the frequency band of the modulation instability narrows down to zero. However, when the pulse propagates and reaches the values of $\partial|A|/\partial\tau \to \infty$ at its front, the pulse spectrum dramatically broadens (Fig. 2), and the approximation of small harmonic perturbation of the permanent solutions used in deriving previous relations becomes inadequate. As a result, at the junction of the pulse fronts, a region of the modulation instability is formed and a soliton-like pulse with a peak power of A_s^2 and duration $\Delta\tau \ll \tau_0$ is generated. The quantities A_s^2 and $\Delta\tau$ can be expressed through the approximate relation

$$R|D|A_\mathrm{s}^2 - \left(\frac{D}{\Delta\tau}\right)^2 - \mu^2 A_\mathrm{s}^4 = 0,$$

which in the $\mu \to 0$ limit undergoes a transition into the definition of the fundamental soliton $RA_\mathrm{s}^2 = D/\Delta\tau^2$.

These qualitative relations are confirmed by the numerical solution of equation (4) for different values of self-steepening μ and anomalous dispersion ($D < 0$). Figure 3 shows the results of numerical simulations of the propagation of a pulse with an amplitude $A_0(t) = \sqrt{P_0}\cosh(\tau/\tau_0)$, duration $\tau_0 = 25$ ps and power $P_0 = 192$ W in a waveguide with the specified values of the parameters D, μ and R.

The data of Figs 3a–c confirm the conclusion that when a pulse propagates in a waveguide with anomalous dispersion, large values of the nonlinearity dispersion prevent the development of the modulation instability. At sufficiently large μ,

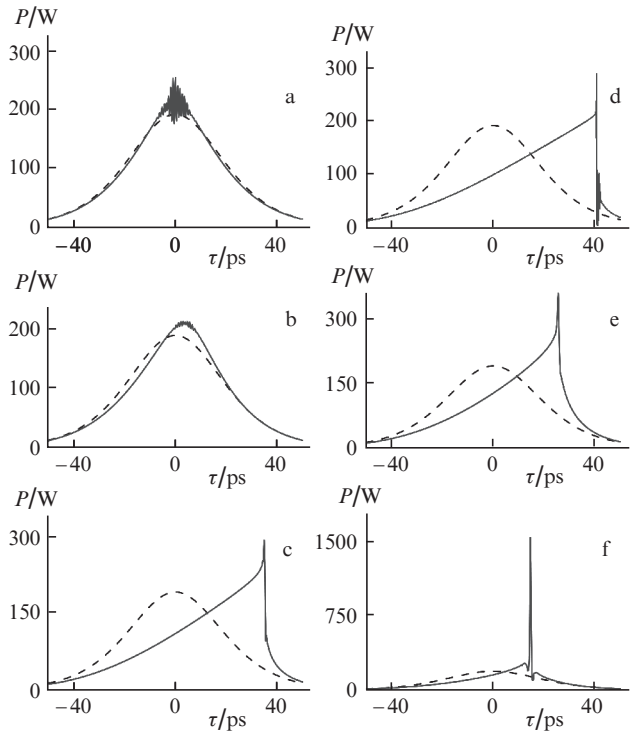

Figure 3. Simulation results of pulse propagation in a waveguide of length l = 5.7 m with (a–c) the parameters R = 0.03 $W^{-1}\,m^{-1}$, D = -3×10^{-25} $s^2\,m^{-1}$, μ = (a) 0, (b) 10^{-15} and (c) 10^{-14} $W^{-1}\,m^{-1}\,s$, as well as in waveguides with (d–f) the parameters R = 0.03 $W^{-1}\,m^{-1}$, μ = 10^{-14} $W^{-1}\,m^{-1}\,s$, (d) $D = -10^{-25}$ $s^2\,m^{-1}$, l = 7.2 m, (e) $D = -10^{-24}$ $s^2\,m^{-1}$, l = 4 m and (f) $D = -5\times10^{-24}$ $s^2\,m^{-1}$, l = 2.4 m. The dashed curves are the envelopes of the initial pulse.

a characteristic multi-peak structure of the pulse is not formed; however, the envelope becomes asymmetric. At a certain propagation length one can observe on the steep edge of the pulse the formation of a single peak. Figures 3d–f show the structure of a pulse with a peak at different anomalous dispersions of the waveguide. One can see that the peak power and the energy of the emerging peak increase with increasing anomalous dispersion of the waveguide, which can be explained by the growth of the modulation gain. This eventually leads to an increase in the ratio of the peak pulse energy to the pedestal energy and at giant values of dispersion ($|D| \sim 10^{-23}$ $s^2\,m^{-1}$) makes it possible to efficiently shorten the initial pulse.

Note also the change in the propagation velocity of the envelope maximum in relation to the velocity at the edge of the pulse on which it is formed. With increasing power, this maximum accelerates (or decelerates, depending on the sign of μ) and penetrates 'inside' the pulse. Thus, the front structure is formed. This process is illustrated by the simulation results given in Fig. 4. It is seen that for large values of $\partial|A|^2/\partial\tau$, a modulation instability region is produced, with the highest value of the modulation gain being reached at the point corresponding to the slope maximum. Due to a lower velocity of the maximum, this region is shifted inside the pulse, leaving behind it a perturbed site. Depending on the ratio of the pulse and waveguide parameters, this process can either be stable or be accompanied by an increase in the frequency range of the modulation instability and by a sharp spectral broadening of the pulse. Finally, the second variant leads to disintegration of the pulse.

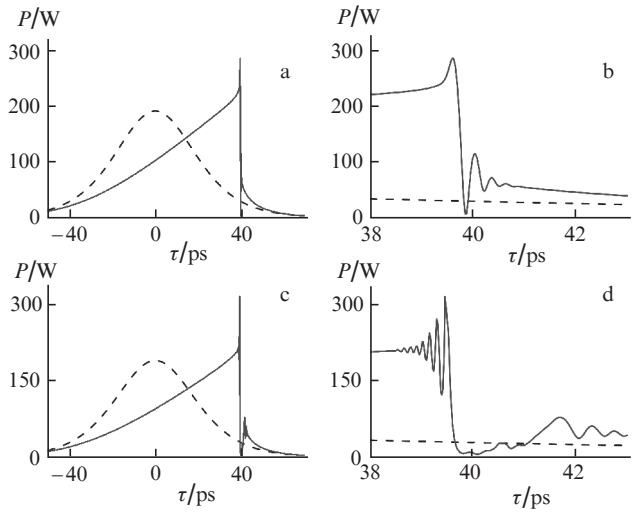

Figure 4. Simulation results of pulse propagation in a waveguide with the parameters R = 0.03 $W^{-1}\,m^{-1}$, $D = -1.5\times10^{-25}$ $s^2\,m^{-1}$, μ = $10^{-14}\,W^{-1}\,m^{-1}\,s$, and l = (a, b) 6.6 and (c, d) 7.5 m. The dashed curves are the envelopes of the initial pulse.

The analysis performed shows that the propagation of radiation pulses in waveguides with large values of the self-steepening parameter μ is of considerable practical interest. Such waveguides may serve as a basis in designing highly efficient optoelectronic elements: compressors, broad-spectrum emitters and pulse generators with a high power gradient. In the next section we discuss the issues related to the possibility of fabricating such waveguides.

4. Value of the self-steepening parameter in gradient waveguides

As was shown above, the dynamics of the radiation pulse is largely dependent on the magnitude and sign of self-steepening μ, characterising the waveguide medium. Typically, this parameter is assumed small and always positive with a very good degree of accuracy equal to $\sim 2R/\omega_0$. Besides, it has little effect on the dynamics of the wave packet in the case when the pulse duration is much larger than 100 fs, whereas the peak power is much less than 1 MW. The above is indeed valid for silica step-index fibres or for recently widely used fibres with a W-shaped refractive index profile. On the other hand, in modern PC waveguides, radiation is localised due to the Bragg mechanism of radiation 'locking' in the fibre core rather than due to the total internal reflection. Obviously, in this case we deal with a strong dependence of the effective mode area and, as a result, of the self-steepening parameter and cubic (Kerr) nonlinearity on the carrier frequency.

Expression (5) defining the self-steepening parameter can be rewritten as

$$\mu = \frac{2n^{(2)}}{cS_{\text{eff}}} - \frac{k_0}{S_{\text{eff}}}\left(\frac{\partial n^{(2)}}{\partial\omega}\right) + \frac{k_0 n^{(2)}}{S_{\text{eff}}^2}\left(\frac{\partial S_{\text{eff}}}{\partial\omega}\right), \qquad (15)$$

where $k_0 = \omega_0/c$. Usually, in analysing the dynamics of the wave packet, the second and third terms in (15) are neglected, which is valid for the most common waveguides with a step or a W-shaped refractive index profile. On the other hand, Zolotovskii and Sementsov [30] showed that in Bragg fibres

with a one-dimensional refractive-index inhomogeneity one can obtain effective values of the self-steepening parameter, which exceed significantly the standard values. Also possible is the realisation of the waveguides with negative μ. The effects of this kind, related to a sharp increase in the magnitude and a change in the sign of the self-steepening parameter, can be observed in the PC waveguides with a two-dimensional refractive index structure. In addition, as a waveguide medium with a large (in modulus) value of the self-steepening parameter we can single out the media with a strong Kerr-nonlinearity dispersion, such as composite materials, described by the Maxwell–Garnett relation [18].

It should be noted that a strong dispersion of the mode area is associated with the instability of a propagating wave packet at which even slight fluctuations in the medium parameters lead to a dramatic increase in optical loss. Thus, the spectral ranges in which the self-steepening parameter has large values are, as a rule, not used due to their strong sensitivity to parameter variations, resulting in significant optical loss. However, for PC media with large cubic nonlinearities in the respective ranges, the shape of the pulse envelope can be effectively controlled.

Consider a typical case by the example of which we can demonstrate the significant dependence of self-steepening on the waveguide parameters – a waveguide with a parabolic profile. The refractive index of the core of a 'standard' waveguide is described by the relation [29]

$$n(r) = n_1\left[1 - \Delta\left(\frac{r}{r_0}\right)^g\right]^{1/2},\ 0 \leqslant r \leqslant r_0, \tag{16}$$

and the refractive index of the cladding – by the relation

$$n(r) = n_1(1-\Delta)^{1/2},\ r \geqslant r_0,$$

where $\Delta = (n_1^2 - n_2^2)/n_1^2$; and n_1 and n_2 are refractive indices of the fibre material. When $g = 1$, the waveguide has a triangular profile of the refractive index, and when $g = 2$, – parabolic. Larger values of g correspond to a step-index waveguide.

To find the dispersion dependences of the fundamental mode parameters of the waveguide, we will solve the wave equation (3) in the Gaussian approximation [29]. The radial distribution of the mode field can be written as

$$U(r) = \exp[-r^2/(2w^2)],$$

where $w = (S_{\text{eff}}/\pi)^{1/2}$ is the mode field radius. The propagation constant is related to the radial distribution of the mode and the refractive index by the expression

$$\beta^2 = \frac{\int_0^\infty [k^2 n^2(r)\, U^2 - (\mathrm{d}U/\mathrm{d}r)^2] r\mathrm{d}r}{\int_0^\infty U^2 r\mathrm{d}r}, \tag{17}$$

where $k = k_0 n_1$. From the equation $\partial\beta^2/\partial w = 0$, we obtain the dispersion dependence of the mode radius:

$$w^2 = 2r_0/(k\sqrt{\Delta}). \tag{18}$$

Thus, the effective area of the waveguide mode $S_{\text{eff}} = 2\pi r_0/(k\sqrt{\Delta})$. Evaluating the integrals in (17), we obtain an expression for the propagation constants of the LP_{01} modes in a waveguide with a parabolic refractive index profile:

$$\beta = k\left(1 - \frac{2\sqrt{\Delta}}{kr_0}\right)^{1/2}.$$

Since $\Delta \ll 1$, then in solving the formulated problem we can assume that $\beta = k_0 n_1$, and therefore the group velocity and GVD do not depend on the waveguide diameter and are constant throughout its length. In this case, for the waveguide with a parabolic refractive index distribution we can write an expression for the Kerr nonlinearity coefficient

$$R = k_0^2 n^{(2)} \sqrt{\Delta}/(2\pi r_0)$$

and the self-steepening parameter [according to (15)]

$$\mu = \frac{k_0\sqrt{\Delta}}{\pi r_0 c}\left(n_1 n^{(2)} - \omega_0 n_1 \frac{\partial n^{(2)}}{\partial\omega} - \omega_0 n^{(2)} \frac{\partial n_1}{\partial\omega} - \frac{\omega_0 n_1 n^{(2)}}{\Delta}\frac{\partial\Delta}{\partial\omega}\right). \tag{19}$$

Note that even in the case under study, the self-steepening parameter μ may differ significantly from the standard value $\sim 2R/\omega_0$ due to the presence of dispersion terms. The sign of μ can be either positive or negative.

Unlike parabolic waveguides, the widely used step-index waveguides have a weak dispersion of the mode area. One can compare their dispersion characteristics by using Marcuse's formula [32]. This formula accurately describes the dependence of the waveguide mode radius w on the waveguide parameter V:

$$\frac{w}{r_0} \approx \frac{A}{V^{2/(2+g)}} + \frac{B}{V^{3/2}} + \frac{C}{V^6}, \tag{20}$$

where

$$V = \frac{\omega r_0}{c}(n_1^2 - n_2^2)^{1/2}.$$

For a step-index waveguide $g \to \infty$, and the numerical coefficients in (20) are defined as $A = 0.65$, $B = 1.619$ and $C = 2.879$. Its dispersion dependence is shown by the dotted curve in Fig. 5. One can see that in the region of 'working' values $r_0 > 2\lambda$ for such waveguides $w \sim r_0$. Comparing this result with (18), we note that the dispersion of the mode area in step-index waveguides is virtually absent (the dependence of the mode area on k is absent).

Consider now a waveguide with a cross-sectional structure that is typical of a PC waveguide. As is shown in [33], Marcuse's formula (20) also describes the dispersion dependence of the mode area. In this case, the waveguide parameter should be defined as

$$V_{\text{PCF}} = \frac{2\pi\Lambda}{\lambda}(n_1^2 - n_{\text{eff}}^2)^{1/2},$$

where n_{eff} is the effective refractive index of the structured cladding of the waveguide. Consider a typical example of a PC fibre (see inset in Fig. 5). The central part of the fibre serving as its core is surrounded by a cladding with a hexagonal system of air holes with a diameter d, separated from each other by a distance Λ. Formula (20) with the coefficients $A_{\text{PCF}} = 0.7078$, $B_{\text{PCF}} = 0.2997$, $C_{\text{PCF}} = 0.0037$, and $g = 8$ provides a

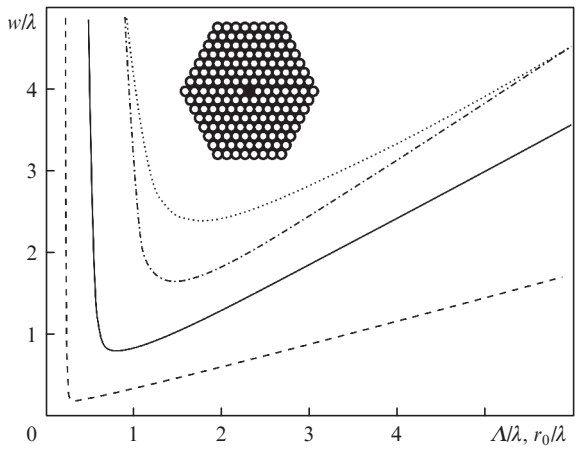

Figure 5. Effective radius of the waveguide mode in a silica structured fibre as a function of a constant structure Λ calculated by using approximation (21) for Λ = 1 μm, d/Λ = (dash-dotted curve) 0.3, (solid curve) 0.5 and (dashed curve) 0.9. The dotted curve is the dependence of the effective radius of the waveguide mode on the core radius r_0 for a standard step-index fibre with $n_1 - n_2 = 0.01$. The inset shows the cross-section of the PC fibre (the figure is borrowed from [34]).

high accuracy of approximation of the dependence of the ratio w/Λ on the parameter $V_{\rm PCF}$:

$$\frac{w}{\Lambda} \approx \frac{A_{\rm PCF}}{V_{\rm PCF}^{2/(2+g)}} + \frac{B_{\rm PCF}}{V_{\rm PCF}^{3/2}} + \frac{C_{\rm PCF}}{V_{\rm PCF}^{6}}. \qquad (21)$$

Figure 5 (borrowed from [34]) shows the dependences of the mode radius on the constant Λ for PC fibres with a hexagonal structure at different values of the d/Λ ratio. Note that the region of the dispersion dependence of the mode radius ($w \propto \Lambda^l$, $l \neq 1$) is within the admissible limits for modern PC waveguides implementing the radiation localisation through the Bragg mechanism. With increasing porosity of the cladding structure, this region is displaced towards the Λ values of the order of wavelength at $d/\Lambda \sim 0.5$. Therefore, one should pay attention to the fact that in the spectral regions near the Bragg matching, the dispersion of the effective mode area can be very strong. Note also that on the left of the point corresponding to the minimum area of the mode, there is a region of a large and thus negative dispersion of the mode area, i.e., $-\partial S_{\rm eff}/\partial\omega \gg S_{\rm eff}/\omega$. Because of the strong change in the mode area and the associated sharp increase in optical loss, the corresponding spectral range is rarely used; however, as we see, it can be used to fabricate waveguides with a giant (in modulus) nonlinearity dispersion. In this range, the self-steepening parameter of PC waveguides can take both positive and negative values that are more than two-to-three orders of magnitude larger in modulus than the standard values.

5. Conclusions

We have studied the dynamics of optical pulses in waveguides characterised by a large value of the self-steepening parameter μ. The urgency of this paper is related to the fact that the evolution of the pulse envelope in such waveguides leads to the emergence of waves with a large power gradient, which are in demand for a wide range of applications. We have considered in detail the process of formation of the shock wave of the envelope at the leading edge (at $\mu < 0$) and the trailing edge ($\mu > 0$) of the pulse both in the absence and in the presence of normal and anomalous dispersion of the waveguide. We have shown that for a large self-steepening parameter the modulation instability of pulses propagating in a nonlinear medium with anomalous dispersion decreases; however, in the region of the highest power gradient this nonlinear effect leads to the formation of soliton-like peaks. Thus, in the case of strong anomalous dispersion we can speak about effective shock compression of the pulse and the achievement of high peak radiation powers. The considered shock-wave mechanism can also find application in the generation of radiation with a broad spectrum.

We have also shown the possibility of realising a waveguide regime with a large (in modulus) positive and negative self-steepening parameter. This regime can be obtained in PC waveguides at wavelengths close to the parameter of the PC fibre cladding structure.

Acknowledgements. This work was supported by the Ministry of Education and Science of the Russian Federation.

References

1. Ostrovsky L.A. *Zh. Tekh. Fiz.*, **33**, 905 (1963) [*Sov. Phys. Tech. Phys.*, **8**, 679 (1964)].
2. Ostrovskii L.A. *Zh. Eksp. Teor. Fiz.*, **51**, 1189 (1966) [*Sov. Phys. JETP*, **24**, 797 (1967)].
3. Mestdagh D., Haelterman M. *Opt. Commun.*, **61**, 291 (1987).
4. Anderson D., Lisak M. *Phys. Rev. A*, **27**, 1393 (1983).
5. Agrawal G.P., Headley C. III. *Phys. Rev. A*, **46**, 1573 (1992).
6. Gromov E.M., Talanov V.I. *Zh. Eksp. Teor. Fiz.*, **110**, 137 (1996) [*JETP*, **83**, 73 (1996)].
7. De Oliveira J.R., de Moura M.A., Hickmann J.M., Gomes A.S.L. *J. Opt. Soc. Am. B*, **9**, 2025 (1992).
8. Zhong W.P., Luo H.J. *Chin. Phys. Lett.*, **17**, 577 (2000).
9. Afanas'ev A.A., Volkov V.M., Urbanovich A.I. *Kvantovaya Elektron.*, **30**, 1002 (2000) [*Quantum Electron.*, **30**, 1002 (2000)].
10. Zolotovskii I.O., Sementsov D.I. *Kvantovaya Elektron.*, **35**, 419 (2005) [*Quantum Electron.*, **35**, 419 (2005)].
11. Wan W., Jia S., Fleischer J. *Nat. Phys.*, **3**, 46 (2007).
12. Tempea G., Brabec T. *Opt. Lett.*, **23**, 762 (1998).
13. Zheltikov A.M. *Usp. Fiz. Nauk*, **170**, 1203 (2000) [*Phys. Usp.*, **43**, 1125 (2000)].
14. Agrawal G., Kivshar Yu. *Optical Solitons. From Fibers to Photonic Crystals* (San Diego: Acad. Press, 2003; Moscow: Nauka, 2005).
15. Zheltikov A.M. *Optika mikrostrukturirovannykh volokon* (Optics of Microstructured Fibres) (Moscow: Nauka, 2004).
16. Smith D.R., Padilla W.J., Vier D.C., Nemat-Nasser S.C., Schultz S. *Phys. Rev. Lett.*, **84**, 4184 (2000).
17. Bilotti F., Tricarico S., Vegni L. *IEEE Trans. Nanotechnol.*, **9**, 55 (2010).
18. Moiseev S.G., Ostatochnikov V.A., Sementsov D.I. *Kvantovaya Elektron.*, **42**, 557 (2012) [*Quantum Electron.*, **42**, 557 (2012)].
19. Basov N.G., Letokhov V.S. *Dokl. Akad Nauk SSSR*, **167**, 77 (1966).
20. Kryukov P.G., Letokhov V.S. *Usp. Fiz. Nauk*, **99**, 169 (1969) [*Sov. Phys. Usp.*, **12**, 641 (1970)].
21. Dysthe K., Krogstad H.E., Muller P. *Annu. Rev. Fluid Mech.*, **40**, 287 (2008).
22. Akhmediev N., Pelinovsky E. *Eur. Phys. J. Special Topics*, **185**, 1 (2010).
23. Didenkulova I., Pelinovsky E. *Nonlinearity*, **24**, R1 (2011).
24. Soomere T. *Eur. Phys. J. Special Topics*, **185**, 81 (2010).
25. Kibler B., Fatome J., Finot C., Millot G., Dias F., Genty G., Akhmediev N., Dudley J.M. *Nat. Phys.*, **6**, 790 (2010).

26. Wabnitz S., Finot C., Fatome J., Millot G. *arXiv 1301*, 0888 (2013).
27. Agrawal G. *Nonlinear Fiber Optics* (CA, San Diego: Academic Press, 2001; Moscow: Mir, 1996).
28. Akhmanov S.A., Vysloukh V.A., Chirkin A.S. *Optics of Femtosecond Laser Pulses* (New York: AIP, 1991; Moscow: Nauka, 1988).
29. Snyder A.W., Love J.D. *Optical Waveguide Theory* (New York: Chapman and Hall, 1983; Moscow: Radio i Svyaz', 1987).
30. Zolotovskii I.O., Sementsov D.I. *Opt. Spektrosk*., **99**, 994 (2005) [*Opt. Spectrosc*., **99**, 957 (2005)].
31. Zolotovskii I.O., Lapin V.A., Sementsov D.I. *Phys. Wave Phenom.*, **21**, 20 (2013).
32. Marcuse D. *J. Opt. Soc. Am.*, **68**, 103 (1978).
33. Nielsen M.D., Mortensen N.A., Folkenberg J.R., Bjarklev A. *Opt. Lett.*, **28**, 2309 (2003).
34. Zheltikov A.M. *Pis'ma Zh. Eksp. Teor. Fiz.*, **91**, 410 (2010).